Electron Paramagnetic Resonance and Optical Spectroscopic Evidence for Interaction between Siroheme and Fe_4S_4 Prosthetic Groups in *Escherichia coli* Sulfite Reductase Hemoprotein Subunit†

Peter A. Janick‡ and Lewis M. Siegel*

ABSTRACT: The hemoprotein subunit (SiR-HP) of *Escherichia coli* NADPH–sulfite reductase contains one siroheme (high-spin Fe^{3+}, D = 8 cm^{-1}) and one oxidized Fe_4S_4 center per polypeptide. Christner et al. [Christner, J. A., Munck, E., Janick, P. A., & Siegel, L. M. (1981) *J. Biol. Chem. 256*, 2098–2101] have shown by Mossbauer spectroscopy that the two prosthetic groups of SiR-HP are magnetically exchange coupled in the oxidized enzyme, a result which indicates the presence of a chemical bridge between them. Photoreduction of SiR-HP in the presence of 5′-deazaflavin and ethylenediaminetetraacetic acid causes the enzyme to accept up to 2.0 electrons. The two reducible centers in SiR-HP are reduced independently with a midpoint potential difference of 65 mV, the siroheme being more positive. The first electron added to SiR-HP results in loss of the g = 6.63, 5.24, and 1.98 set of EPR signals due to the ferriheme and production of an EPR-silent state. The second added electron results in the parallel appearance of three distinct types of EPR signal: a novel species with g = 2.53, 2.29, and 2.07 (0.63 spin per heme); two "$S = {}^3/_2$ type" species with g = 5.23, 2.80, and ca. 2.0 and g = 4.82, 3.39, and ca. 2.0 (together account for 0.16 spin per heme); and a very small amount of a "classical" reduced Fe_4S_4 center signal with g = 2.04, 1.93, and 1.91 (0.03 spin per heme). The temperature dependences of the "g = 2.29" and "g = 1.93" signals are similar to each other and are like those seen with other Fe_4S_4 center proteins. Addition of small amounts of guanidinium sulfate (0.1 M) to SiR-HP causes the spectrum of fully reduced enzyme to show primarily the $S = {}^3/_2$ type species (g = 4.88, 3.31, and 2.08; 0.84 spin per heme), although the enzyme remains fully active. Optical spectral changes followed as a function of enzyme reduction show that marked changes occur in the Fe^{2+} siroheme optical spectrum when the Fe_4S_4 center becomes reduced or oxidized. These results indicate that the prosthetic groups of SiR-HP remain coupled when the enzyme is reduced. It is suggested that the novel EPR signals result from exchange interaction between S = 1 or 2 ferroheme and $S = {}^1/_2$ reduced Fe_4S_4.

Escherichia coli NADPH–sulfite reductase (SiR)[1] is a complex hemoflavoprotein (M_r 685 000; subunit structure $\alpha_8\beta_4$) capable of catalyzing the six-electron reductions of SO_3^{2-} to S^{2-} and NO_2^- to NH_3 (Siegel et al., 1973, 1982; Siegel & Davis, 1974). As isolated, the NADPH–SiR complex contains a multiplicity of prosthetic groups: four FAD, four FMN, four Fe_4S_4 centers, and 4 mol of a novel iron tetrahydroporphyrin termed siroheme (Siegel et al., 1973; Murphy et al., 1973; Siegel, 1978). Scott et al. (1978) have determined the complete stereochemical structure of siroheme and found it to be an iron dimethylurotetrahydroporphyrin of the isobacteriochlorin type (i.e., adjacent pyrrole rings reduced). Siroheme also serves as a prosthetic group in assimilatory nitrite reductases from higher plants (Murphy et al., 1974) as well as in other assimilatory and dissimilatory sulfite reductases (Murphy & Siegel, 1973; Krueger & Siegel, 1982a).

The siroheme-containing subunits of *E. coli* NADPH–SiR can be separated from the flavin-containing subunits by treatment of the enzyme with 4 M urea followed by DEAE-celulose chromatography (Siegel & Davis, 1974). The hemoprotein subunit (SiR-HP), as isolated, is a monomeric polypeptide, M_r 54 000, containing 1 mol of siroheme and one Fe_4S_4 center (Siegel et al., 1982). While the flavoprotein portion of the native SiR complex is required for NADPH-dependent SO_3^{2-} reduction, the artificial electron donor reduced methylviologen will support stoichiometric reduction of SO_3^{2-} to S^{2-} catalyzed by the hemoprotein alone (Siegel et al., 1982). Indeed, in reviewing the structure of sulfite and nitrite reductases from a variety of sources, Siegel (1978) has noted that the catalytic apparatus required for the six-electron reduction reactions catalyzed by both enzymes is remarkably simple: a polypeptide of M_r 50 000–70 000 containing one siroheme and one Fe_4S_4 center as prosthetic groups. In both types of enzyme, the active polypeptide binds 1 mol of substrate or 1 mol of an inhibitory ligand, such as cyanide, at the heme (Lancaster et al., 1979; Siegel et al., 1982). CN^- or CO binding to the heme precludes the binding of substrate.

Although some initial studies on reduction of *E. coli* SiR hemoflavoprotein by NADPH have been reported (Siegel & Kamin, 1968), it has been difficult to obtain substantial reduction of the enzyme Fe_4S_4 center with this reductant. Reduced methylviologen, a reductant of more negative reduction potential than NADPH, is unsuited for optical studies of the enzyme. As reported by Siegel et al. (1982), it is also difficult to achieve substantial Fe_4S_4 center reduction with this agent as well. Although dithionite, the classical strong reductant used in enzymology, can be used to reduce Fe_4S_4 centers of SiR in which the heme is ligated to inhibitors such as CN^- or CO (Siegel et al., 1982), this agent cannot be used to reduce unligated SiR since it gives rise to SO_3^{2-} upon electron transfer to the enzyme, and a $S_2O_4^{2-}$-dependent re-

† From the Department of Biochemistry, Duke University School of Medicine, and the Veterans Administration Hospital, Durham, North Carolina 27705. *Received February 3, 1982.* This work was supported by Grant AM-13460 from the National Institutes of Health, Grant PCM-7924877 from the National Science Foundation, and Project Grant 7875-01 from the Veterans Administration.

‡ This work is part of a dissertation submitted by P.A.J. to Duke University in partial fulfillment of the requirements for the degree of doctor of philosophy. P.A.J. is a fellow of the Medical Scientist Training Program at Duke University.

[1] Abbreviations: Dfl, 5′-deazaflavin; Fe_2S_2, Fe_3S_3, and Fe_4S_4, binuclear, trinuclear, and tetranuclear iron–sulfur centers, respectively; SiR, sulfite reductase; SiR-HP, hemoprotein subunit of *E. coli* NADPH–sulfite reductase; EDTA, ethylenediaminetetraacetic acid.

0006-2960/82/0421-3538$01.25/0

duction of SO_3^{2-} ensues in which the enzyme is in a turnover state which contains relatively little reduced Fe_4S_4 (Siegel et al., 1973, 1982).

Massey & Hemmerich (1978) have described the use of a photochemical reducing system of very negative reduction potential to reduce flavin, heme, and iron–sulfur-containing enzymes. In this system, EDTA serves as reductant for a photoactivated 5′-deazaflavin (Dfl) molecule, converting the latter to a strongly reducing Dfl radical species. When the light is turned off, the Dfl radicals rapidly react to form a stable dimer species. Use of this technique has permitted us to achieve complete reduction of SiR holoenzyme and its HP subunit in both free and inhibitor complexed states. This paper reports the appearance of novel EPR and optical spectral species of the uncomplexed enzyme on reduction. These spectra indicate the presence of interaction between the siroheme and Fe_4S_4 centers in fully reduced SiR-HP and suggest that the strong exchange coupling detected between these centers in oxidized SiR-HP by Mossbauer spectroscopy (Christner et al., 1981) is maintained as the enzyme is reduced.

Experimental Procedures

Materials. NADPH–SiR holoenzyme was purified from *E. coli* B by the procedure of Siegel et al. (1973). The SiR-HP subunit was dissociated from the holoenzyme by using 4 M urea and isolated by DEAE-cellulose chromatography as described by Siegel & Davis (1974). The isolated SiR-HP was extensively dialyzed vs. 0.1 M potassium phosphate–0.1 mM EDTA, pH 7.7, buffer to remove the urea. This "standard buffer" was used in all experiments unless otherwise indicated. All buffers were prepared by using triply distilled water and were passed over a Chelex-100 column to remove extraneous Fe and other trace metals. SiR-HP concentration was measured spectrophotometrically by using the E_{591} = 18 mM^{-1} cm^{-1} reported by Siegel et al. (1982). Dfl was a generous gift from Dr. David Seibert. Aqueous solutions of Dfl were prepared and concentrations determined spectrophotometrically as described by Massey & Hemmerich (1978).

Photoreduction of SiR-HP. Reduction of SiR-HP was achieved with the procedure of Massey & Hemmerich (1978). In the experiments reported in this paper, 10 mM EDTA and Dfl/SiR-HP ratios of 0.20 were used. However, complete reduction of enzyme could be accomplished (although at a slower rate) with Dfl/SiR-HP ratios of 0.1 and EDTA concentrations of 1 mM. Cuvettes or EPR tubes containing anaerobic enzyme–Dfl–EDTA solutions were placed in a chromatography tank filled with ice–water (to prevent overheating) and subjected to periods of illumination with a General Electric 200-W "narrow spot" sealed beam lamp. At intervals, the samples were removed from the bath and optical spectra recorded to follow the progress of the reduction. Complete reduction required illumination periods of as little as 2 min or as much as 120 min depending on the absorbance of the SiR-HP solution (enzyme concentration and path length of cuvette or EPR tube).

Due to the low potential of the reducible centers in SiR-HP and the inherent reactivity of the reduced centers with O_2, rigorous anaerobiosis was essential, and all experiments were performed under Ar atmospheres. Residual O_2 was removed from the Ar (Matheson, high purity) by passing the gas successively, in an all glass system, through a BASF copper catalyst column (heated to 190 °C) and then through a solution of concentrated reduced methylviologen.

Optical studies were performed on solutions contained in a specially constructed "double cuvette" consisting of a quartz spectrophotometer cell (1-cm path length) fused to a male ground glass joint that would accommodate a stopper designed to fit a 2-mL Becton-Dickinson vaccutainer tube. When a needle was inserted through the stopper, this lower portion could be connected to the gas line and the solution made anaerobic by repeated evacuation and flushing with Ar. A top with two gas taps connected to a female ground glass joint provided a gas-tight cap for the apparatus. One gas tap with a fused ground glass ball joint allowed connection to the gas line so that the top section could be evacuated and filled with Ar. The second gas tap, arranged parallel to the cuvette, was occluded with a serum stopper, and 0.8 mL of concentrated methylviologen solution was layered over the vaccutainer stopper to minimize O_2 diffusion into the opical cell. Additions to the cuvette were made from a gas-tight syringe (Glenco) by inserting a 9-in. needle through both stoppers.

Samples to be analyzed by EPR were photoreduced in EPR tubes with fused quartz male ground glass joints. A top was constructed with two female ground glass joints arranged in parallel: one to connect to the EPR tube and the second to provide an entry port. Perpendicular to these two female joints was a gas tap with a ground glass ball joint, which allowed the apparatus to be connected to the gas line. Solutions were made anaerobic in Thunberg tubes and were transferred anaerobically to the EPR tubes by means of gas-tight syringes previously evacuated and flushed with Ar.

Recording and Analysis of Spectra. Optical spectra were recorded with an Aminco DW-2 dual-beam spectrophotometer by using either 1-cm path-length quartz cuvettes or EPR tubes (average effective path length, measured with reduced cytochrome *c*, was 0.32 cm). EPR tubes were positioned in the light path by means of a holder in the bottom of the sample compartment, and an Aminco microcondenser accessory was used to collimate the light beam. Since the light was further focused by the cylindrical faces of the EPR tube, spectra of high quality were obtained, although the absolute positioning of the spectrum base line was highly sensitive to slight changes in positioning of the EPR tube in the light path. So that this problem (which led to the entire spectrum moving up or down without any changes in its shape) could be corrected for during the monitoring of reduction of SiR-HP samples in EPR tubes, the observed absorbance at 626 nm was corrected for base-line shifts by subtracting the observed absorbance at 760 nm (a wavelength where little change occurred on reduction) from each spectrum. The resulting quantity was normalized by dividing it by the $A_{591}-A_{760}$ of the oxidized material in the EPR tube prior to reduction; this corrected for differences in effective path length of each EPR tube. By use of this quantity, the number of electrons present in a specific partially reduced enzyme sample could be readily determined by interpolation on a standard curve constructed from $Fe(CN)_6^{3-}$ back-titrations of enzyme which had been photoreduced in standard cuvettes.

EPR spectra were recorded at X band with a Varian E-9 spectrometer equipped with a liquid helium cryostat (Air Products). Temperature was measured by using a thermocouple calibrated with a 5 K Ω carbon resistor. Modulation frequency was 100 KHz and modulation amplitude 10 G in all experiments. Spin concentrations were determined from spectra recorded under nonsaturating conditions either by double integration or by integration of isolated absorption-type peaks by the method of Aasa & Vanngard (1975); CuEDTA served as standard. The following temperature and microwave powers were used for quantitative measurements of the various EPR signals described in this paper: "g = 6.63" species (high-spin ferriheme), 20 K, 50 mW; "g = 4.82" and "g =

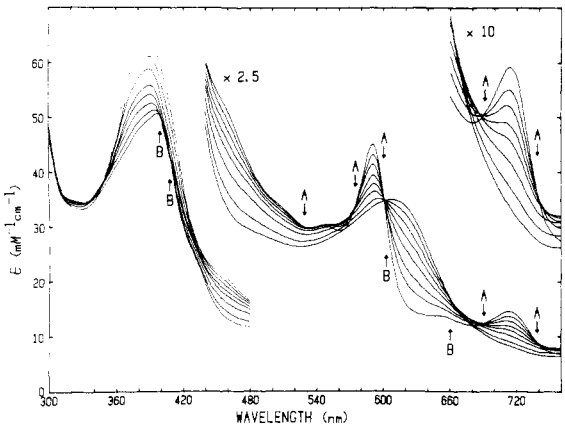

FIGURE 1: Optical spectra of SiR-HP during photoreduction with Dfl–EDTA. A solution containing 24 μM SiR-HP, 5 μM Dfl, and 10 mM EDTA in standard buffer was made anaerobic in the double-cuvette apparatus and illuminated for 0.5–1-min intervals as described under Experimental Procedures. The final period of illumination was extended to 3 min and the optical spectrum recorded, and then the solution was further illuminated for 3 min, and the observed spectrum was found not to change. The initial set of spectra observed during photoreduction yielded the set of isosbestic points labeled A, while the final set of spectra yielded the set of isosbestic points labeled B. The oxidized enzyme exhibits its α-band maximum at 591 nm, while the reduced enzyme spectrum shows a broad α band centered about 608 nm.

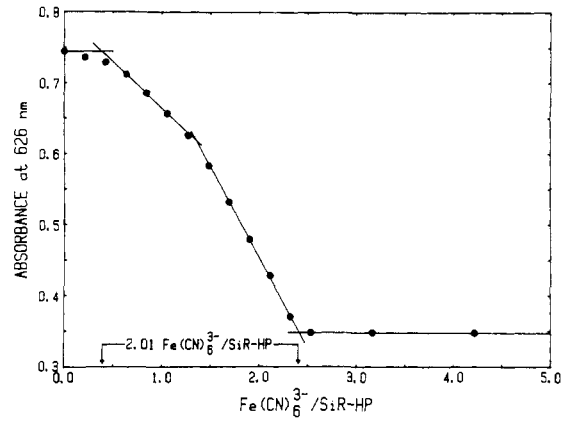

FIGURE 2: Titration of fully reduced SiR-HP with ferricyanide. A solution containing 59.6 μM SiR-HP, 12 μM Dfl, 10 mM EDTA, 15 ng/mL bovine liver catalase (Worthington), and 30 ng/mL bovine superoxide dismutase in standard buffer, total volume 0.5 mL, was made anaerobic in the double-cuvette apparatus. A needle fitted to a gas-tight syringe containing 3.153 mM $K_3Fe(CN)_6$ in standard buffer was inserted into the apparatus, and the enzyme was then photoreduced until no further change in the optical spectrum occurred (20 min). Aliquots of ferricyanide were then added, and the optical spectrum was recorded after each addition. The absorbance at 626 nm was corrected for dilution by the added ferricyanide solution and plotted as a function of ferricyanide added.

5.23" species, 8 K, 100 mW; "g = 2.29" species, 20 K, 50 mW; "g = 1.93" species, 20 K, 10 mW. A Hewlett-Packard 9825A computer equipped with 9874A digitizer and 7225A graphics plotter was used for integration and simulations of EPR spectra and for calculation of derived optical spectra. EPR spectral simulations were performed by using the program of Lowe (1978).

Theoretical curves for the variation of EPR signal intensity (S) as a function of microwave power (P) were calculated by using the semiempirical equation given by Beinert & Orme-Johnson (1967):

$$\log (S/\sqrt{P}) = \text{constant} - 0.5b \log (1 + P/P_{1/2})$$

where $P_{1/2}$ = the microwave power at half-saturation and b, the "inhomogeneity parameter", varies from 1.0 for inhomogeneously broadened lines to 4.0 for the homogeneous case.

Results

Optical Spectra. Absorption spectra obtained after various periods of photoreduction of SiR-HP in the presence of Dfl–EDTA are shown in Figure 1. The spectrum of the oxidized enzyme is dominated by the high-spin ferriheme absorbance with wavelength maxima at 388, 547, 591, and 714 nm. [Extinction coefficients for oxidized SiR-HP have been given by Siegel et al. (1982).] The initial stages of reduction lead to decreases in absorbance in the Soret and 714-nm band regions and broadening of the α band (591-nm peak) with isosbestic points labeled A in Figure 1 (528, 577, 600, 695, and 738 nm). As photoreduction continues, this set of isosbestic points is lost, and a new set of isosbestic points, labeled B in Figure 1 (402, 408, 602, and 660 nm), appears as reduction nears completion. The spectrum of the fully reduced enzyme is characterized by a Soret band at 397 nm (E = 49.0 mM^{-1} cm^{-1}) and a very broad α band at 608 nm (E = 14.2 mM^{-1} cm^{-1}). There is an increase in absorbance in the wavelength region between 528 and 575 nm during the initial phases of reduction. The absorbance in this region declines, however, as reduction proceeds. These results are consistent with an enzyme-reduction process which involves two sequential but partially overlapping reductive events.

Fully reduced SiR-HP could be readily reoxidized by stepwise addition of small amounts of $Fe(CN)_6^{3-}$. The same spectral species were observed during the course of both photoreduction of SiR-HP and its reoxidation with $Fe(CN)_6^{3-}$, and the spectrum of fully oxidized enzyme was completely regenerated upon addition of excess $Fe(CN)_6^{3-}$. Two sets of isosbestic points were observed during the reoxidation; these were identical with sets B and A seen on reduction. When the reoxidation of photoreduced SiR-HP by $Fe(CN)_6^{3-}$ was followed at 626 nm, a wavelength yielding substantial absorbance changes in all phases of the reaction, results like those shown in Figure 2 were obtained.

The change in A_{626} showed a "lag" phase on addition of the first amounts of $Fe(CN)_6^{3-}$. [Control experiments involving illumination of the Dfl–EDTA solution in the absence of enzyme have shown that the photoreducing system itself produces a reproducible number of $Fe(CN)_6^{3-}$-reactive reducing equivalents. These equivalents are more reactive with $Fe(CN)_6^{3-}$ than is the reduced enzyme, and this accounts for the lag phenomenon observed when absorbance changes in the enzyme are measured in oxidative titrations with $Fe(CN)_6^{3-}$. The number of these equivalents could be reduced to about 20 μM by inclusion of small amounts of catalase and bovine superoxide dismutase in the standard photoreduction system. The relative effect of these "low-potential" equivalents in titration experiments could be minimized by use of high enzyme concentrations.]

Subsequent to the lag, two nearly linear phases of absorbance change were observed, each phase involving the uptake of 1 mol of $Fe(CN)_6^{3-}$ per mol of SiR-HP. Because of the lag phenomenon, the extent of the first linear phase of enzyme reoxidation could only be determined accurately by back-extrapolation of the first linear portion of the A_{626} vs. [$Fe(CN)_6^{3-}$] titration curve (corrected for dilution) to the initial A_{626} of the fully reduced enzyme sample. In contrast, the end point of the titration was invariably sharp. Five independent $Fe(CN)_6^{3-}$ titrations, of which that shown in Figure 2 is one, were performed by using three different concentrations (24, 24, 39, 60, and 60 μM) of photoreduced SiR-HP. When

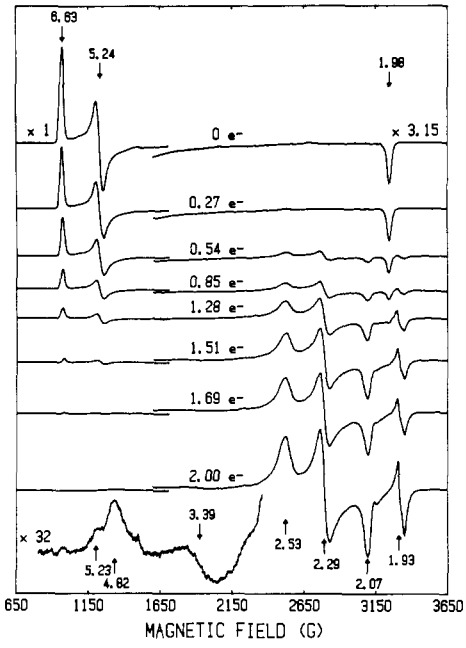

FIGURE 3: EPR spectra at 20 K of photoreduced SiR-HP. Anaerobic solutions containing 210 μM SiR-HP, 40 μM Dfl, and 10 mM EDTA in standard buffer were illuminated in anaerobic EPR tubes for times between 0 and 100 min. The extent of reduction in each tube was determined from the optical spectrum as described in the text. EPR spectra were recorded at microwave frequency 9.12 GHz, 50-mW microwave power, and at a temperature of 20 K. The high-field portion of the spectra was recorded by using an instrument gain 3.15 times that used for the low-field portion. The high-field portion of the spectra for the 1.51-, 1.69-, and 2.00-electron-reduced samples has been displaced slightly upward for the sake of clarity. The bottom magnified spectrum of the low-field region in the 2.00 electron reduced enzyme sample was run at 200-mW power at a relative gain of 32.

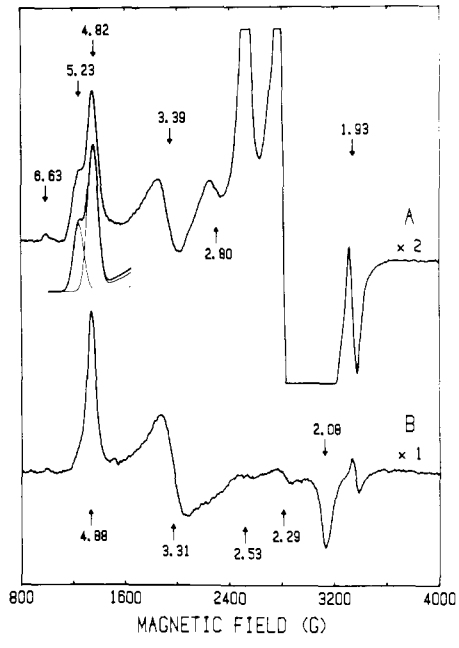

FIGURE 4: EPR spectra at 8 K and high microwave power of fully reduced SiR-HP in the absence and presence of guanidinium sulfate. (A) A solution containing 210 μM SiR-HP was photoreduced to full reduction as described in Figure 3. Below the spectrum is shown a simulation of the low-field feature as the sum of two Gaussian peaks with line widths of 28 G and $g = 5.23$ and $g = 4.82$ in a ratio of 0.8:1.0. (B) A solution containing 72 μM SiR-HP, 15 μM Dfl, 10 mM EDTA, and 0.1 M guanidinium sulfate in standard buffer was photoreduced to full reduction (15 min of illumination). The optical spectra of the photoreduced enzyme samples were identical (when corrected for the difference in enzyme concentration). EPR spectra were recorded at 9.12-GHz microwave frequency, 8 K temperature, and 100-mW microwave power.

corrected for the amount of $Fe(CN)_6^{3-}$ used in the lag phase, these titrations show that a total of 1.99 ± 0.03 mol of $Fe(CN)_6^{3-}$ per mol of SiR-HP was required for complete reoxidation of the fully reduced enzyme. We can conclude that the spectral changes exhibiting the isosbestic set A on photoreduction involve addition of a first electron to SiR-HP, while the changes exhibiting the isosbestic set B on photoreduction involve addition of a second electron to the enzyme.

EPR Spectra. EPR spectra of SiR-HP at various stages of reduction were obtained by illuminating anaerobic EPR tubes containing solutions of SiR-HP and Dfl–EDTA. The extent of enzyme reduction in each sample was measured optically, and the sample was then frozen in liquid N_2 for EPR analysis. The characteristic $S = {}^5/_2$ high-spin ferriheme EPR signal ($g = 6.63$, 5.24, and 1.98) of oxidized SiR-HP integrated to 0.92 spin per heme at 7 K. As shown in Figure 3, the initial stages of enzyme reduction involve loss of this ferriheme signal. With continued reduction, a new EPR signal with $g = 2.53$, 2.29, and 2.07 appears and increases in intensity as reduction proceeds to completion. In parallel with this latter signal, another set of resonances arises with distinct features observed at $g = 5.23$ and 2.80 and $g = 4.82$ and 3.39 (Figures 3 and 4). These g values, split about $g = 4$, suggest that these resonances represent two separate species with possible $S = {}^3/_2$ ground states. (These "$S = {}^3/_2$" type signals are best observed at very low temperatures, 5–10 K, and high microwave power settings; they are not in fact easily detected, except in highly concentrated samples of reduced SiR-HP, at 20 K and 50 mW power, the standard conditions for observing the $g = 2.29$ set of EPR signals.) A third type of EPR signal, of the classical $g = 1.94$ type characteristic of reduced Fe_4S_4 centers in a number of iron–sulfur proteins, with $g = 2.04$, 1.93, and 1.91, of low intensity also arises more or less in parallel with the $g = 2.29$ and $S = {}^3/_2$ type signals on enzyme reduction.

Assignment of g values for the various $S = {}^3/_2$ type species has been facilitated by our finding that low concentrations of guanidinium sulfate or KCl added to reduced SiR-HP greatly increased the intensity of the $S = {}^3/_2$ type EPR signals at the expense of the $g = 2.29$ species. As seen in Figure 4, the EPR spectrum of fully reduced SiR-HP in standard buffer containing 0.1 M guanidinium sulfate is dominated by a sharp signal at $g = 4.88$, 3.31, and 2.08, which integrates to 0.84 spin per heme. In the presence of 5 mM KCl (data not shown), at least two distinct $S = {}^3/_2$ type species of similar g value are produced, one of which is broad and the other is quite sharp with $g = 5.30$, 2.71, and ca. 2.0. The perturbation of the reduced SiR-HP spectra by these and other agents will be further discussed in a subsequent publication. It is clear from these spectra that the g_3 features of the $S = {}^3/_2$ type signals seen in the presence of guanidinium sulfate or KCl are located at or above $g = 2.0$. In the native SiR-HP, the lack of significant absorbance below $g = 2.0$ under conditions where the $g = 1.93$ signal is highly saturated indicates that the g_3 features of the EPR signals associated with the resonances at $g = 5.23$ and $g = 4.82$ in the native reduced enzyme are likewise to be found at $g \geq 2.0$, although the presence of resonances due to the $g = 2.29$ species prevents a precise determination of this g value by direct visualization of the spectra.

Quantitation of the various types of EPR signals seen in fully reduced SiR-HP showed that the $g = 2.29$ signal represented the majority reduced species, accounting for 0.63 spin per heme. The $g = 1.93$ signal represents a relatively minor

species, accounting for only 0.03 spin per heme. (The relatively narrow line width of the $g = 1.93$ signals in comparison to those for the other reduced SiR-HP EPR signals makes this species appear to be more prominent in observed spectra than it really is in terms of spin concentration.) Integration of the $S = {}^3/_2$ type signals was complicated by the overlap of the g_1 features of the two observed signals. By use of the EPR simulation program of Lowe (1978), two Gaussian peaks of line width 28 G with g values of 5.23 and 4.82 were combined as shown in Figure 4. Using the peak area of the g feature for each of the simulated signals, one could estimate the spin concentrations of the $g = 5.23$ and $g = 4.82$ signals to be 0.07 and 0.09 spin per heme, respectively.

Taken together, the spin concentration of all the signals seen in fully reduced SiR-HP represents 0.82 spin per heme. Greatly prolonging the period of illumination of the enzyme samples did not increase the total spin concentration of reduced centers. The ratio of the various signals was essentially constant in reduced enzyme samples from SiR-HP preparations prepared from three independently grown samples of *E. coli* B; it was also unchanged in enzyme samples which had previously undergone a cycle of photoreduction and reoxidation by $Fe(CN)_6^{3-}$. Given the difficulty of accurately quantitating an overlapping group of EPR signals, we do not consider the value of 0.82 spin per heme for the reduced enzyme centers to be significantly different from the value of 1.0 spin per heme expected on the basis on the $Fe(CN)_6^{3-}$ titration data.

The EPR data of Figure 3 and Mossbauer data of Christner et al. (1981) are in agreement that the first electron taken up by SiR-HP is accommodated by the siroheme moiety, the Fe_4S_4 center remaining oxidized. The Mossbauer data clearly show that the second electron is taken up by the Fe_4S_4 center. Thus, the $g = 2.29$, $g = 4.82$, and $g = 5.23$ EPR signals, as well as the more classical type of $g = 1.93$ signal, are associated with reduction of the Fe_4S_4 center in enzyme in which the heme is in the ferrous state. In SiR-HP ligated by CN^- or CO, only a standard $g = 1.94$ type of EPR signal is seen on full reduction of the enzyme, this signal accounting for nearly 1 spin per heme (Siegel et al., 1982). In such ligated enzyme, the ferrous heme is expected to be low spin ($S = 0$), so that there is no ready means for magnetic interaction between the $S = {}^1/_2$ reduced Fe_4S_4 center and the reduced heme. In the "free" SiR-HP, however, the ferrous heme is probably magnetic ($S = 1$ or 2; Christner et al., 1981), and perturbation of the reduced Fe_4S_4 center EPR spectrum might well be expected if there is substantial interaction between the reduced heme and Fe_4S_4 centers. The presence of such markedly perturbed EPR signals in the spectra of Figures 3 and 4 strongly indicates that there is magnetic interaction between these centers in the fully reduced SiR-HP and suggests that the exchange coupling between prosthetic groups demonstrated by Christner et al. (1981) for oxidized SiR-HP by Mossbauer spectroscopy is maintained as the enzyme becomes reduced.

Electron Distribution in Reduced SiR-HP. Each optical spectrum obtained during the course of reoxidation of fully reduced SiR-HP with $Fe(CN)_6^{3-}$ could be assigned to an enzyme species containing a given number of electrons which corresponded to the amount of $Fe(CN)_6^{3-}$ required to convert that state to the fully oxidized enzyme (after taking into account the lag phenomenon of Figure 2). The absorbance change at 660 nm (isosbestic point from set B, Figure 1) was used to follow the reduction state of the first photoreducible center (siroheme), while the absorbance change at 528 nm (isosbestic point from set A, Figure 1) was used to follow the reduction state of the second center (Fe_4S_4). The results,

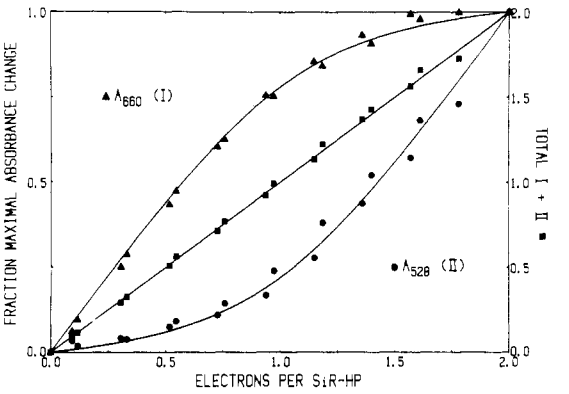

FIGURE 5: Distribution of electrons in prosthetic groups of SiR-HP: optical spectra. Two ferricyanide titrations of solutions containing 59.6 μM fully photoreduced SiR-HP were performed as described in Figure 2. Each spectrum recorded during the reoxidation was assigned a number of electrons per heme based on the calibration curve of Figure 2 (this subtracts the amount of ferricyanide consumed in the lag phase of the titration). The absorbance at 660 and 528 nm was measured for each titration point, corrected for dilution, and normalized to the total absorbance change between fully reduced and fully oxidized enzyme observed at each of these wavelengths. (▲) Fractional absorbance change at 660 nm. This wavelength, one of the isosbestic points labeled B in Figure 1, measures changes in oxidation state of the first enzyme group to be photoreduced (I), the ferriheme. (●) Fractional absorbance change at 528 nm. This wavelength, one of the isosbestic points labeled A in Figure 1, measures changes in oxidation state of the second enzyme prosthetic group to be photoreduced (II), the Fe_4S_4 center. (■) Sum of the fractional changes in I and II. The theoretical curves (solid lines) are based on Scheme I and assume a 65-mV difference in midpoint potential between two independent centers I and II, each exhibiting ideal Nernstian $n = 1$ reduction behavior (for details see the text).

Scheme I

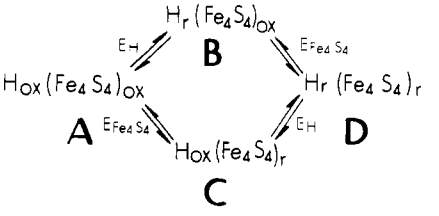

shown in Figure 5, closely fit a theoretical distribution (solid lines) of electrons between two independently reducible centers in equilibrium with each other and following ideal Nernstian $n = 1$ reduction behavior with a 65 mV difference in midpoint potential between the two centers. The model used to calculate the theoretical distribution is shown in Scheme I. The fraction of enzyme to be found in each of the species $H_{ox}(Fe_4S_4)_{ox}$, $H_{ox}(Fe_4S_4)_{red}$, $H_{red}(Fe_4S_4)_{ox}$, and $H_{red}(Fe_4S_4)_{red}$ was calculated from the following equations:

$$[H_{red}(Fe_4S_4)_{red}]/[HP]_{total} = [1 + 10^{(2E-E_H-E_{Fe4S4})/59} + 10^{(E-E_{Fe4S4})/59} + 10^{(E-E_H)/59}]^{-1}$$

$$[H_{ox}(Fe_4S_4)_{ox}]/[HP]_{total} = ([H_{red}(Fe_4S_4)_{red}]/[HP]_{total})[10^{(2E-E_H-E_{Fe4S4})/59}]$$

$$[H_{ox}(Fe_4S_4)_{red}]/[HP]_{total} = ([H_{red}(Fe_4S_4)_{red}]/[HP]_{total})[10^{(E-E_{Fe4S4})/59}]$$

$$[H_{red}(Fe_4S_4)_{ox}]/[HP]_{total} = ([H_{red}(Fe_4S_4)_{red}]/[HP]_{total})[10^{(E-E_H)/59}]$$

where H refers to siroheme, red and ox refer to reduced and oxidized states of each carrier, HP refers to SiR hemoprotein subunit, E = solution potential, E_H = midpoint potential of siroheme (Fe^{3+}/Fe^{2+}), and $E_{Fe_4S_4}$ = midpoint potential of Fe_4S_4

center (ox/red). In Figure 5, the theoretical curve for the first photoreducible center (I) = $[H_{red}(Fe_4S_4)_{ox} + H_{red}(Fe_4S_4)_{red}]/[HP]_{total}$ and that for the second photoreducible center (II) = $[H_{ox}(Fe_4S_4)_{red} + H_{red}(Fe_4S_4)_{red}]/[HP]_{total}$. The total number of electrons present in SiR-HP at any given solution potential would theoretically be equal to

$$[2 + 10^{(E-E_{Fe4S4})/59} + 10^{(E-E_H)/59}]/[1 + 10^{(2E-E_H-E_{Fe4S4})/59} + 10^{(E-E_{Fe4S4})/59} + 10^{(E-E_H)/59}]$$

The solution potential is used as an independent parameter to calculate the electron distributions in the various enzyme forms as a function of the number of electrons in the enzyme for the theoretical curves of Figures 5 and 6. The solid squares in the center of Figure 5 correspond to the sum of the fractional amounts of the optical changes associated with each of the two enzyme centers on reduction. The fact that the sum of these fractional changes plotted as a function of electrons in the enzyme [from $Fe(CN)_6^{3-}$ titration] is a straight line between the values zero and two electrons per SiR-HP indicates that these changes do indeed account well for the overall reduction state of the enzyme.

EPR can also be used to determine the electron distribution by measuring the intensity of the ferriheme and reduced Fe_4S_4 center EPR signals as a function of the number of electrons in photoreduced SiR-HP samples determined optically from the absorbance at 626 nm (using calibration curves like that in Figure 2). In view of the diversity of EPR signals present in the fully reduced enzyme, each of the three major types (represented by the $g = 2.29$, $g = 4.82$, and $g = 1.93$ signals, respectively) of signal seen in the fully reduced enzyme was handled separatedly. Overlap of most of the $S = {}^3/_2$ type signal resonances with those of the ferriheme or $g = 2.29$ signals precluded accurate quantitation of all but the g_2 ($g = 3.39$) feature of the $g = 4.82$ species. Thus, we could follow the $g = 4.82$ but not the $g = 5.23$ species as a function of enzyme reduction state. However, we found that there was no drastic change in the intensity of the observable portion of the $g = 2.80$ resonance associated with the $g = 5.23$ species in relation to the intensity of the $g = 3.39$ resonance as reduction proceeded. Thus, the two types of $S = {}^3/_2$ species seem to be reduced together, within experimental error. The observed distribution of the various signals as a function of electrons in the enzyme is shown in Figure 6. The theoretical curves of that figure were drawn assuming ideal Nernstian reduction behavior of the two centers, with the Fe_4S_4 center being 65 mV more negative in potential than the siroheme. The theoretical curve for the $g = 6.63$ EPR signal in Figure 6 assumes that the signal is derived only from the species $H_{ox}(Fe_4S_4)_{ox}$, while all of the other states of Scheme I are EPR silent at this resonance. The theoretical curve for the reduced Fe_4S_4 signals assumes that the signals at $g = 2.29$, $g = 4.82$, and $g = 1.94$ derive only from the species $H_{red}(Fe_4S_4)_{red}$ and that the other states of Scheme I are EPR silent at these resonances. Thus, the minority species $H_{ox}(Fe_4S_4)_{red}$, as well as the majority one-electron species $H_{red}(Fe_4S_4)_{ox}$, is assumed to be EPR silent. It is important to note that despite the small amount of $H_{ox}(Fe_4S_4)_{red}$ which should be present if the two centers are indeed reduced independently but differ in potential by 65 mV (a maximum of 4% of the enzyme would ever be expected to be in this form), it was found to be impossible to fit both the optical data of Figure 5 and the EPR data of Figure 6 with a common value for the potential difference between the centers unless this assumption is made. This result in itself is suggestive of spin coupling and hence magnetic interaction between the siroheme and Fe_4S_4 prosthetic groups in one-electron reduced SiR-HP.

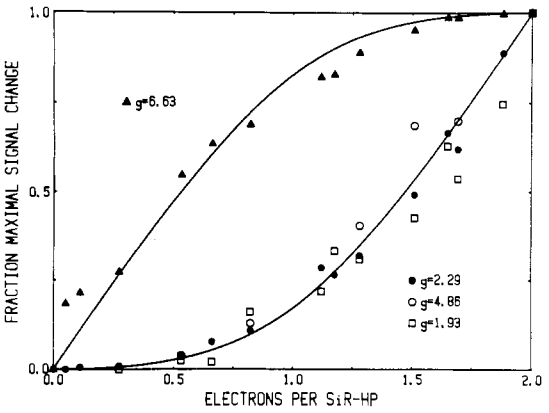

FIGURE 6: Distribution of electrons in prosthetic groups of SiR-HP: EPR spectra. Anaerobic solutions of SiR-HP in EPR tubes were photoreduced as described in Figure 3 and the number of electrons present in the enzyme determined from the optical spectrum as described in the text. EPR signals for the $g = 6.63$ (ferriheme), $g = 2.29$, $g = 1.93$, and $g = 4.82$ species were measured and quantitated as described in the text. For each EPR species, the amount of signal present has been divided by the maximum amount of signal seen (in oxidized enzyme for the $g = 6.63$ species, in fully enzyme for the other signals). (▲) One fraction of $g = 6.63$ signal found in oxidized enzyme; (●) fraction of maximum $g = 2.29$ signal; (□) fraction of maximum $g = 1.93$ signal; (○) fraction of maximum $g = 4.82$ species. The theoretical curves (solid lines) are based on Scheme I and assume that there are two independently reducible centers in the enzyme, separated in potential by 65 mV, the first center giving rise to the $g = 6.63$ signal (when oxidized) and the second center giving rise to any of the other signals (when reduced). For details see the text. The experimental points for the $g = 6.63$, $g = 2.29$, and $g = 1.93$ species were obtained with solutions containing both 24 and 210 μM SiR-HP. The points for the $g = 4.82$ species were measured only on the solutions containing 210 μM SiR-HP.

In Figure 6, the fractional degree of reduction of the $g = 2.29$ EPR signal is plotted as a function of electrons in the enzyme. Similarly, the fractional reductions of the $g = 4.82$ and $g = 1.93$ are plotted. In each case, the signal behaves as if it can represent the total amount of Fe_4S_4 EPR signal as a function of enzyme reduction state. Thus, to a first approximation, we can conclude that each of the reduced EPR species present is due to a center 65 mV more negative in potential than the siroheme.[2]

Optical Spectrum of SiR-HP Containing One Electron. As the midpoint potentials of the heme and Fe_4S_4 centers are relatively close, intermediate stages of enzyme reduction usually involve mixtures of the various enzyme oxidation states shown in Scheme I. Thus, one cannot obtain in solution spectra of pure SiR-HP species containing only one electron. However, the optical spectrum of this form [largely $H_{red}(Fe_4S_4)_{ox}$, as shown by Mossbauer spectroscopy (Christner et al., 1981), but containing a small amount of $H_{ox}(Fe_4S_4)_{red}$] can be approximated by extrapolation of the absorbance changes at a large number of wavelengths associated with the linear portions of $Fe(CN)_6^{3-}$ titrations of reduced enzyme like that shown in Figure 2. Although the absorbance change due to addition of the first fraction of an electron to SiR-HP results largely from reduction of the heme, there is a small amount

[2] Accurate theoretical fits to the titration data of Figure 6 show that the $g = 4.82$ species and $g = 1.93$ species behave as if they have potentials slightly more positive (+5 mV) or more negative (−10 mV), respectively, than that of the $g = 2.29$ species. The siroheme populations corresponding to the three signal types seen in fully reduced enzyme need not have exactly the same midpoint potentials. However, since the different populations of siroheme cannot be separated in the data of Figure 6, it is evident that any differences in siroheme population potentials must be small.

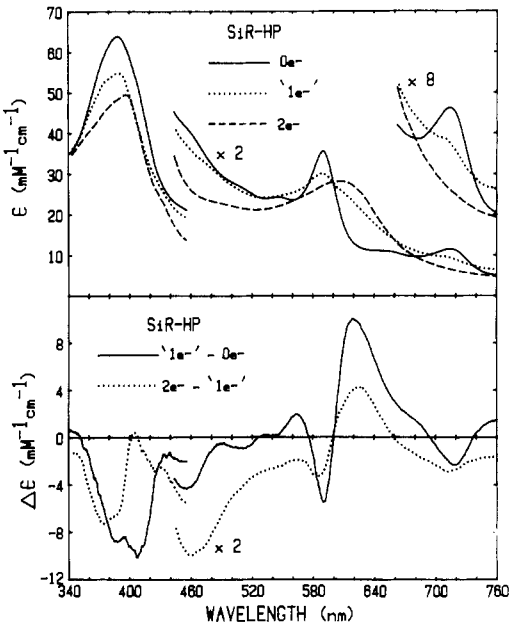

FIGURE 7: Optical spectra of SiR-HP in states containing 0, 1, and 2 electrons and difference spectra between successive enzyme oxidation states. The optical spectra obtained during the later stages of two ferricyanide titrations involving 60 μM photoreduced SiR-HP and two involving 24 μM photoreduced SiR-HP (less than 0.7 electron per heme) were digitized (one point/nm) with the Hewlet-Packard digitizer. At each wavelength the absorbance (corrected for enzyme concentration) as a function of the number of electrons present in the enzyme was extrapolated to a value of 1.0 electron by a least-squares fit of the data in a linear regression program. The resulting spectrum was then used to determine a preliminary difference spectrum between the 1.0- and 2.0-electron-reduced forms of the enzyme. The extrapolation was then corrected for contaminating amounts of the 2.0-electron enzyme by subtracting off the calculated contribution of the latter species at each wavelength, assuming a 65-mV difference in potential between reducible enzyme centers and Scheme I. This correction led to a slightly modified spectrum for the 1.0-electron form and a slightly altered difference spectrum between the 1.0- and 2.0-electron forms of the enzyme. The correction procedure and extrapolation were then repeated. The resulting spectrum for 1.0-electron enzyme species did not change on further application of the correction and extrapolation procedure. (Top panel) Optical spectra of oxidized (—), 1.0-electron-reduced (···), and 2.0-electron-reduced (- - -) species of SiR-HP. (Bottom panel) Difference spectra between 1.0-electron-reduced SiR-HP and oxidized SiR-HP (—) and between 2.0-electron-reduced SiR-HP and 1.0-electron-reduced SiR-HP.

of enzyme which has been reduced by two electrons as well. So that this contribution could be corrected for, a series of successive approximations of the extrapolation were performed (see legend to Figure 7 for details) to obtain a more accurate optical spectrum of the one-electron reduction state of SiR-HP. As seen in Figure 7, addition of one electron to the enzyme results in decreased absorbance in the Soret region, with a decline in absorbance and a broadening of the α-band maximum of oxidized SiR-HP. The charge-transfer peak at 714 nm associated with the high-spin ferriheme state of siroheme both in oxidized SiR-HP and in model siroheme complexes (Stolzenberg et al., 1981) is also lost [although a slight shoulder persists in this region, perhaps indicative of a small amount of $H_{ox}(Fe_4S_4)_{red}$ species present]. As the second electron enters the enzyme, the decline in absorbance in the Soret region continues, with the Soret band shifting to 397 nm in the fully reduced enzyme. Although there is generally a decline in absorbance in the region between 410 and 500 nm as the second electron is added to SiR-HP, there are substantial and complex changes in the α-band region, with a major shift in this now rather broad band to 608 nm and markedly increased absorbance between 600 and 650 nm. Thus it is

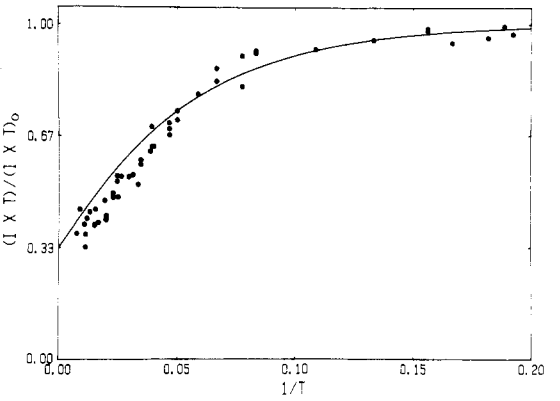

FIGURE 8: Temperature dependence of the high-spin ferriheme EPR signal. The intensity (I) of the $g = 6.63$ feature of the high-spin ferriheme signal in oxidized SiR-HP, measured by means of the low-field half peak area of this feature, was normalized for microwave power and instrument gain (spectra were measured under nonsaturating conditions in all cases) and the result multiplied by the absolute temperature (T, in K). The value of IT_0 used to normalize the data was obtained by the best fit of the low temperature points, although the results were not significantly different if the value of IT determined at the lowest temperatures measured was used as $(IT)_0$. The solid line gives the temperature dependence predicted for an $S = {}^5/_2$ system with $D = 8$ cm^{-1} using the equation given in the text.

evident that addition of *each* electron to SiR-HP results in complex spectral changes of the type generally associated with changes in hemes rather than Fe_4S_4 centers.

Temperature Dependence of the High-Spin Ferriheme EPR Signal. The EPR signal of the siroheme in oxidized SiR-HP is characteristic of an $S = {}^5/_2$ system with substantial rhombic distortion. Such a system can be described by the spin Hamiltonian:

$$H = \beta g_0 HS + D[S_z^2 - S(S+1)/3 + (S_x^2 - S_y^2)E/D]$$

The term in D arises from the zero field splitting of the $S = {}^5/_2$ sextet into three Kramers doublets $\pm{}^1/_2$, $\pm{}^3/_2$, and $\pm{}^5/_2$, of which only the $\pm{}^1/_2$ doublet is EPR detectable for $E/D \ll {}^1/_3$. Under these conditions the upper doublets lie $2D$ and $6D$ (the correction for $E/D > 0$ is second order and thus less than 0.1% for SiR-HP) above the ground state $S_z = \pm{}^1/_2$ doublet. Since population of the three doublets follows a Boltzmann distribution, the fraction of the center in the EPR active lowest Kramers doublet (N_T/N_0) is given by

$$N_T/N_0 = (IT)/(IT)_0 = [1 + e^{-2D/(kT)} + e^{-6D/(kT)}]^{-1}$$

where I represents the signal intensity at temperature T and the subscript zero refers to measurements taken at or near absolute zero. Figure 8 shows the temperature dependence of the integrated intensity of the $g = 6.63$ peak of the high-spin ferriheme signal of SiR-HP. A value of $D = 8 \pm 1$ cm^{-1} yields the best fit of the data by using the above equation (solid line).[3] Above 30 K there is a significant deviation of the data from the theoretical curve (using any resonable value of D). This deviation may reflect loss of EPR signal due to population of additional EPR silent excited states created by the siroheme–Fe_4S_4 interaction in oxidized SiR-HP (Christner et al., 1981).

Properties of the EPR Signals in Fully Reduced SiR-HP. Figure 9 shows the relaxation behavior at 10 K of the three types of EPR signal seen in fully reduced SiR-HP. The theoretical curves were calculated as described under Exper-

[3] An identical value of D has been obtained from analysis of the Mossbauer spectrum of oxidized SiR-HP (Christner et al., 1981).

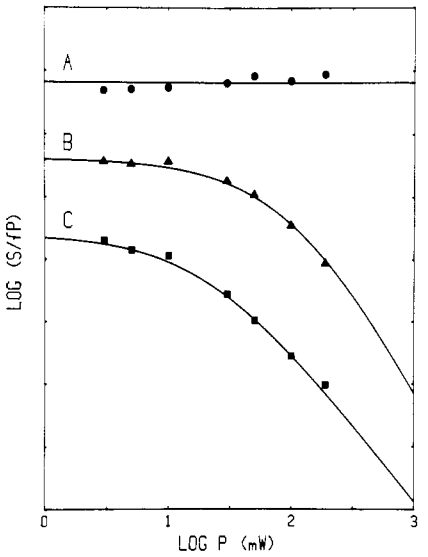

FIGURE 9: Microwave power saturation behavior of EPR signals in fully reduced SiR-HP. A solution containing 210 μM SiR-HP was fully reduced as described in Figure 3. EPR spectra were recorded at 10 K. Signal intensities were measured at the g_2 feature for the $g = 4.86$ species (A) (●) and $g = 1.93$ species (C) (■) and at the g_1 feature for the $g = 2.29$ feature (B) (▲). Units of log (S/P) are arbitrary and are plotted by using the equation and parameters described in the text.

imental Procedures. At this temperature, the $g = 1.93$ signal is readily saturated, with $P_{1/2} = 20$ mW and homogeneity parameter $b = 1$. The $g = 2.29$ species relaxes more rapidly, with $P_{1/2} = 110$ mW ($b = 1.5$), while the $g = 4.86$ species displays very rapid relaxation behavior, precluding evaluation of $P_{1/2}$ at 10 K.

The g values of the $g = 2.29$ species suggest that the effective spin of this species is $S = {}^1/_2$. (The Mossbauer spectrum of the Fe_4S_4 center is consistent with an $S = {}^1/_2$ system spin.[4]) Temperature studies indicated virtually no change in the shape or line width of the signal below 30 K, although above this temperature the signal rapidly broadens and becomes virtually undetectable above 40 K. The large deviation from Curie law dependence of the signal intensity on temperature above 20 K (Figure 10) indicates that the $g = 2.29$ signal does not behave as if it is due to a simple $S = {}^1/_2$ system but that it possesses thermally accessible EPR silent excited states. Such states are characteristic of exchange coupled systems, but for systems with more than two centers the theory describing these excited states is not well understood and further analysis is difficult. (The Fe_4S_4 unit must be considered to consist of four interacting centers, since each iron atom has an electronic spin; addition of an exchange coupled $S = 1$ or 2 ferroheme further complicates the system.) The broadening and loss of signal above 30 K may represent extreme lifetime broadening due to a two-phonon Orbach pathway that becomes thermally accessible at this temperature.[5]

Only a small fraction of the fully reduced SiR-HP gives a $g = 1.93$ EPR signal. As suggested previously (Siegel et al., 1982), this signal may well arise from enzyme species in which magnetic interaction between heme and Fe_4S_4 centers is precluded, perhaps because, as with CN^-- or CO-ligated enzyme, the reduced heme is in an $S = 0$ state. Indeed, if concentrated samples of oxidized SiR-HP are examined by EPR, small amounts of low-spin ferriheme signals, heterogeneous in nature and representing less than 0.05 spin per SiR-HP in total, are found. Rueger & Siegel (1976) have shown that substantial amounts of low-spin ferriheme, representing 10–20% of the total heme, are found in spectra of the NADPH–SiR holoenzyme. We have found, in agreement with the above ideas, that the amount of $g = 1.93$ type EPR signal found in fully reduced holoenzyme correlates closely with the amount of low-spin ferriheme found in the oxidized enzyme.

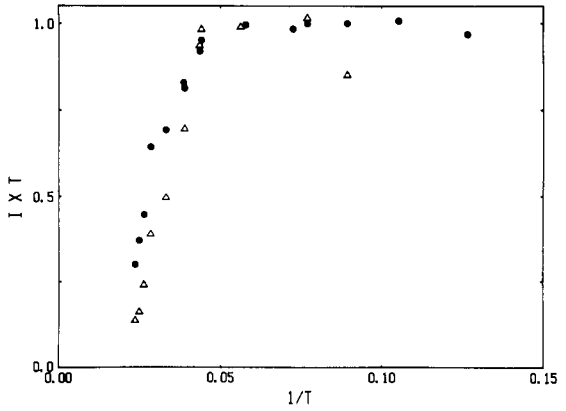

FIGURE 10: Temperature dependence of the $g = 2.29$ and $g = 1.93$ EPR signals in fully reduced SiR-HP. A solution containing 300 μM SiR-HP was fully reduced as described in Figure 3. Signal intensities were measured at nonsaturating power, normalized to constant power and gain, and multiplied by absolute temperature, and the result (IT) was normalized by dividing by IT at the lowest temperature examined. (●) $g = 2.29$ species, measured as the double integral; (△) $g = 1.93$ species, measured as amplitude of the g_2 feature.

As shown in Figure 10, the $g = 1.93$ signal shows a temperature dependence very similar to that of the $g = 2.29$ species. Points at very low temperatures could not be obtained for the $g = 1.93$ signal since this signal was highly saturated at the lowest microwave power settings available to us at those temperatures. The rapid loss of signal intensity as the temperature is raised to about 40 K seen in both the $g = 2.29$ and $g = 1.93$ signals is a common characteristic of Fe_4S_4 center proteins (Blum et al., 1979).

The temperature dependences of the two types of $S = {}^3/_2$ signal are similar, with no apparent change in the proportion of these signals as a function of temperature. Plots of the temperature dependence of the integrated signal intensity of the $g = 4.82$ feature (data not shown) indicate a decline in the value of IT with increasing temperature even when the temperature is raised from 5 to 7 K. Above 13 K, the signal rapidly broadens and intensity falls off faster and further (to less than 0.5 the IT at 5 K) than the $[1 + e^{-2D[1+3(E/D)^2]^{1/2}/(kT)}]^{-1}$ dependence expected for a true $S = {}^3/_2$ system, using any value of D.[6] Although population of additional excited states may explain the signal loss, at least some of the decreased intensity may be due to lifetime broadening of the rapidly relaxing $S = {}^3/_2$ type signal.

[4] J. A. Christner, E. Munck, P. A. Janick, and L. M. Siegel, unpublished results.

[5] Blum et al. (1979) have used equations of the form $(IT)/(IT)_0 = [1 + me^{-\Delta/(kT)}]^{-1}$ to fit the temperature dependence of the signal intensity of the HiPiP EPR signal from *Chromatium vinosum* iron–sulfur protein and the $g = 1.94$ type EPR signals from a variety of Fe_4S_4 proteins. Such an equation can be used to fit the high-temperature data obtained with the $g = 2.29$ signal of reduced SiR-HP, but the resulting fit, with multiplicity (m) = 87.5 and energy separation (Δ) = 109 cm^{-1}, is not particularly enlightening at present.

[6] Due to the rapid decay of signal intensity for the $S = {}^3/_2$ type EPR signals of reduced SiR-HP as the temperature is raised, it is difficult to see these signals under the normal conditions for examining the $g = 2.29$ and $g = 1.93$ signals (20 K, 10- or 50-mW power). Thus this class of signal was missed in our preliminary report of the EPR data which accompanied the Mossbauer results of Christner et al. (1981).

Discussion

The $Fe(CN)_6^{3-}$ titrations of fully reduced SiR-HP indicate that two electrons can be accommodated by the enzyme. Mossbauer spectroscopy has shown that the first of these electrons to enter the enzyme primarily reduces the ferriheme, while the second electron is primarily accommodated by the Fe_4S_4 center (Christner et al., 1981). Reduction of the Fe_4S_4 center in ferroheme enzyme results in production of a novel set of EPR signals, involving a majority species with an apparent system spin of $S = {}^1/_2$ and three g values in the range 2.07–2.53, two minority species of *apparent* system spin $S = {}^3/_2$, and only a small amount of the classical $g = 1.94$ type of EPR signal normally associated with isolated reduced Fe_4S_4 centers in iron–sulfur proteins.

The $g = 2.29$ type of signal is not restricted to SiR-HP photoreduced with Dfl–EDTA. We have detected large amounts of the signal in SiR-HP reduced in the presence of a reduced methylviologen-generating system of very negative reduction potential, composed of 9 mM pyruvate, 22 μM CoA, *Clostridium acidiurici* pyruvate dehydrogenase, and 440 μM methylviologen in standard buffer.[7] The signal has also been seen in smaller amounts in *E. coli* NADPH–SiR holoenzyme incubated with 900 NADPH per heme.[7]

Using potentiometric titrations (in the presence of viologen and other dye mediators) coupled to EPR analysis of frozen samples, Siegel et al. (1982) measured the midpoint potential for reduction of the ferriheme in SiR-HP to be −340 mV. We have found a nearly identical potential for the enzyme heme by optical measurements in the presence of safranine T at room temperature,[8] coulometric measurements in the presence of viologen dye mediators at room temperature,[9] and EPR measurements of frozen samples of NADPH–SiR which had been equilibrated with defined mixtures of NADPH and $NADP^+$ at room temperature prior to freezing.[7] From the data of Figures 5 and 6, we can conclude that the Fe_4S_4 center exhibits a reduction potential 65 mV more negative than that of the heme, i.e., −405 mV.

Despite the fact that this potential should yield significant reduction of the Fe_4S_4 centers in SiR-HP in potentiometric titrations in which chemically reduced methylviologen serves as both reductant and mediator, little or no such reduction was observed in experiments reported by Siegel et al. (1982). It now appears that the inability to observe substantial amounts of Fe_4S_4 reduction in such experiments may be due to a significant negative shift in the reduction potential of the SiR-HP Fe_4S_4 center in the presence of methylviologen. Thus, preliminary coulometric titrations of SiR-HP using methylviologen as mediator indicate reduction of a center at a midpoint potential of −450 mV.[9] Also, addition of a solution of 50% reduced methylviologen to photoreduced SiR-HP causes substantial *oxidation* of the reduced Fe_4S_4 centers, as measured by EPR.[8] NADPH titration experiments with NADPH–SiR holoenzyme are consistent with a midpoint potential of approximately −410 mV for the Fe_4S_4 center in that enzyme.[7]

Although the transition from one-electron-reduced SiR-HP to fully reduced enzyme primarily involves reduction of the Fe_4S_4 center in an enzyme in which the heme oxidation state remains constant (as ferrous), the optical as well as the EPR changes associated with this transition are quite unusual when one considers the usual spectral properties of reduced vs. oxidized Fe_4S_4 centers. Thus, proteins containing such centers and $Fe_4S_4(SR)_4^{2-}$ model compounds generally absorb visible light with broad peaks centered about 400 and 450 nm, respectively ($E = \sim 15$ mM^{-1} cm^{-1}), with bleaching of this absorbance on reduction of the cluster (Palmer, 1975; Holm & Ibers, 1976). Reduction of an Fe_4S_4 center therefore would be expected to result in a generalized decrease in absorbance in this region, with quantitatively rather small changes occurring at wavelengths greater than 600 nm. Instead complex optical changes are seen on reduction of the Fe_4S_4 in SiR-HP, with substantial *increases* in absorbance between 600 and 650 nm where only small decreases in Fe_4S_4 center absorbance would normally be expected. It is clear from the difference spectra in Figure 7 that both stages of enzyme reduction markedly perturb the siroheme absorption spectrum. Since there is no change in siroheme oxidation state as the one-electron enzyme is converted to the two-electron enzyme, it is clear that the electronic properties of the siroheme are perturbed when the Fe_4S_4 center changes oxidation state. The novel EPR signals seen in the fully reduced enzyme certainly suggest that the reduced Fe_4S_4 center magnetic properties are affected by the presence of siroheme.

Christner et al. (1981) have demonstrated magnetic splitting of the oxidized ($S = 0$) Fe_4S_4 center Mossbauer spectrum by the paramagnetic ($S = {}^5/_2$) ferriheme in oxidized SiR-HP. Arising from antiferromagnetic exchange between the heme and Fe_4S_4, this interaction implies the existence of a chemical link between the two centers, presumably in the form of a bridging ligand. [See Cohen (1980) for a review of antiferromagnetic exchange coupling in enzyme systems.] The optical and EPR spectral results reported in this paper strongly indicate that such an interaction between the two centers also exists when the enzyme is reduced. This result is of potential importance for our understanding of the catalytic mechanism since Siegel et al. (1974, 1982) have shown that SO_3^{2-} and inhibitory ligands only bind rapidly to SiR when the enzyme has been reduced.

In an attempt to conceptually simplify theoretical investigations of the interaction between the heme and Fe_4S_4 centers in oxidized SiR-HP, Munck (1981) has suggested a model in which the $S = {}^5/_2$ ferriheme is coupled to an oxidized Fe_2S_2 center. In this case the interaction was predicted to have a negligible effect on the g values of the high-spin ferriheme EPR signal since the **g** tensors of the Fe^{3+} atoms in the Fe_2S_2 center would be virtually identical and very close to g_e (as is the heme **g** tensor). Reduction of the coupled system to give an Fe^{2+} siroheme–reduced Fe_2S_2 center presents a more complicated situation. Whether the ferroheme is $S = 1$ or 2 (the two alternatives cannot yet be distinguished since the isomer shift and quadrapole splitting parameters seen in Mossbauer spectra of fully reduced SiR-HP are intermediate between the values normally seen for high-spin $S = 2$ and intermediate spin $S = 1$ ferrous heme model complexes), its Fe^{2+} atom would not be expected to have an isotropic **g** tensor due to contributions from spin–orbit coupling in either case. Theoretical expressions for the **g** tensor as a function of the zero field splitting and spin and spin–orbit coupling for octahedral Fe^{2+} ($S = 2$) in hemoglobin have been given by Lang (1970). The susceptibility data of Nakano et al. (1972) on single crystals of deoxyhemoglobin indicate that the **g** tensor of the heme Fe^{2+} is anisotropic, with g_x and g_y greater than the g_z equal to g_e. When a spin vector model (Sands & Dunham, 1975) is used, coupling schemes that orient the Fe^{2+}–siroheme *and* the Fe^{2+} atom of the coupled Fe_2S_2 center parallel to the system spin will move the **g** tensor of the coupled system to values much larger than $g = 2.0$ with only modest anisotropy of the heme

[7] L. M. Siegel and W. H. Orme-Johnson, unpublished results.
[8] P. A. Janick and L. M. Siegel, unpublished results.
[9] J. A. Spence, M. J. Barber, and L. M. Siegel, unpublished results.

g tensor. If the Fe^{2+}–heme spin alone were responsible for the g values of the coupled center, larger deviations of the heme **g** tensor would be required to produce such changes. While this approach is obviously much oversimplified, it nevertheless allows one to qualitatively appreciate how the **g** tensor of a signal such as that seen in the $g = 2.29$ species of the reduced SiR-HP EPR spectrum could be produced.

The nature of the $S = {}^3/_2$ type EPR signals is unclear at present.[10] It must be emphasized that the $S = {}^3/_2$ spin-state terminology is based solely on the observed g values of the system and that we have been unable to detect any EPR signal that could represent a transition from the $S = \pm{}^3/_2$ upper Kramers doublet. Also, Mossbauer spectroscopy on samples of SiR-HP reduced in the presence of KCl, which contain substantially increased proportions of the $S = {}^3/_2$ EPR signals, has failed to reveal substantial alteration of the native reduced SiR-HP Mossbauer spectrum.[7] This result argues against the possibility that the $g = 2.29$ and $S = {}^3/_2$ type EPR signals derive from different ferroheme spin states coupled to the reduced Fe_4S_4 center spin. Thus, we cannot rule out the very real possibility that the $g = 5.23$ and $g = 4.82$ species arise from an extremely anisotropic $S = {}^1/_2$ system, the shift in g values resulting from changes, for instance, in the magnitude and/or sign of the exchange coupling between the two centers. Such alterations in coupling can result from relatively small changes in bond lengths or angles between atoms in coupled systems (Hatfield, 1976).[11]

Acknowledgments

We are grateful to Patricia Davis for preparing the enzyme used in this work.

References

Aasa, R., & Vanngard, T. (1975) *J. Magn. Reson. 19*, 308–315.

Beinert, H., & Orme-Johnson, W. H. (1967) in *Magnetic Resonance in Biological Systems* (Ehrenberg, A., Malmstrom, B. G., & Vanngard, T., Eds.) pp 221–247, Pergamon Press, Oxford.

Blum, H., Salerno, J. C., Prince, R. C., Leigh, J. S., Jr., & Ohnishi, T. (1979) *Biochim. Biophys. Acta 548*, 139–146.

Christner, J. A., Munck, E., Janick, P. A., & Siegel, L. M. (1981) *J. Biol. Chem. 256*, 2098–2101.

Cohen, I. A. (1980) *Struct. Bonding (Berlin) 40*, 1–37.

Hatfield, W. E. (1976) in *Theory and Applications of Molecular Paramagnetism* (Boudreaux, E. A., & Mulay, L. N., Eds.) pp 349–449, Wiley, New York.

Holm, R. H., & Ibers, J. A. (1976) in *Iron-Sulfur Proteins* (Lovenberg, W., Ed.) Vol. 3, pp 205–281, Academic Press, New York.

Kreuger, R. J., & Siegel, L. M. (1982a) *Biochemistry 21*, 2892–2904.

Kreuger, R. J., & Siegel, L. M. (1982b) *Biochemistry 21*, 2905–2909.

Lancaster, J. R., Vega, J. M., Kamin, H., Orme-Johnson, N. R., Orme-Johnson, W. H., Kreuger, R. J., & Siegel, L. M. (1979) *J. Biol. Chem. 254*, 1268–1272.

Lang, G. (1970) *Q. Rev. Biophys. 3*, 1–60.

Lowe, D. J. (1978) *Biochem. J. 171*, 649–651.

Massey, V., & Hemmerich, P. (1978) *Biochemistry 17*, 9–17.

Munck, E. (1981) in *Iron-Sulfur Biochemistry* (Spiro, T. G., Ed.) Wiley-Interscience, New York.

Murphy, M. J., & Siegel, L. M. (1973) *J. Biol. Chem. 248*, 6911–6919.

Murphy, M. J., Siegel, L. M., Kamin, H., & Rosenthal, D. (1973) *J. Biol. Chem. 248*, 2801–2814.

Murphy, M. J., Siegel, L. M., Tove, S. R., & Kamin, H. (1974) *Proc. Natl. Acad. Sci. U.S.A. 71*, 612–616.

Nakano, N., Otsuka, J., & Tasaki, A. (1972) *Biochim. Biophys. Acta 278*, 355–371.

Palmer, G. (1975) *Enzymes, 3d Ed. 12*, 1–56.

Rueger, D. C., & Siegel, L. M. (1976) in *Flavins and Flavoproteins* (Singer, T. P., Ed.) pp 610–620, Elsevier, Amsterdam.

Sands, R. H., & Dunham, W. R. (1975) *Q. Rev. Biophys. 7*, 443–504.

Scott, A. I., Irwin, A. J., Siegel, L. M., & Shoolery, J. N. (1978) *J. Am. Chem. Soc. 100*, 7987–7994.

Siegel, L. M. (1978) in *Mechanisms of Oxidizing Enzymes* (Singer, T. P., & Ondarza, R. N., Eds.) pp 201–214, Elsevier/North-Holland, New York.

Siegel, L. M., & Kamin, H. (1968) in *Flavins and Flavoproteins* (Yagi, K., Ed.) pp 15–40, University Park Press, Baltimore.

Siegel, L. M., & Davis, P. S. (1974) *J. Biol. Chem. 249*, 1587–1598.

Siegel, L. M., Davis, P. S., & Kamin, H. (1973) *J. Biol. Chem. 248*, 251–264.

Siegel, L. M., Rueger, D. C., Barber, M. J., Kreuger, R. J., Orme-Johnson, N. R., & Orme-Johnson, W. H. (1982) *J. Biol. Chem.* (in press).

Stolzenberg, A. M., Strauss, S. H., & Holm, R. H. (1981) *J. Am. Chem. Soc. 103*, 4763–4778.

[10] EPR signals of the $g = 2.29$ type have been detected in photoreduced samples of assimilatory ferredoxin-SiR from spinach (Krueger & Siegel, 1982b). Signals of both the $S = {}^3/_2$ and $g = 2.29$ type (with the $S = {}^3/_2$ the majority species) have been observed by us in photoreduced samples of spinach ferredoxin–nitrite reductase, an enzyme which also contains siroheme and Fe_4S_4 centers (J. O. Wilkerson, P. A. Janick, and L. M. Siegel, unpublished results). Mossbauer spectra of oxidized spinach nitrite reductase show that the heme and Fe_4S_4 centers are exchange coupled in this enzyme as well. Thus two distinct six-electron reductase enzymes appear to contain the same type of active center.

[11] Several alternative explanations for the $S = {}^3/_2$ type EPR signals have been considered, but these appear to be unsatisfactory. For instance, existence of an $S = {}^3/_2$ Fe^+(I) heme–oxidized Fe_4S_4 species can be ruled out by results of Mossbauer spectroscopy since there is no evidence for 16% of an oxidized Fe_4S_4 center species (corresponding to the 0.16 spin per heme associated with the two $S = {}^3/_2$ species) in fully reduced SiR-HP. The precision of the $Fe(CN)_6^{2-}$ titration data tends to rule out reduction of a similar proportion of the enzyme to a three electron Fe^+(I) heme–reduced Fe_4S_4 form. The $S = {}^3/_2$ signal does not appear to arise from an excited state of the coupled Fe^{2+} heme–reduced Fe_4S_4 center since there is no apparent decline in the plot of EPR signal intensity times temperature as the temperature is lowered. Also, the amount of the $S = {}^3/_2$ state in reduced enzyme can be increased to 0.84 spin per heme with 0.1 M guanidinium sulfate, a much higher population than one would expect for an excited state.